Study on the AC Impedance Spectroscopy for the Li Insertion Reaction of $Li_xLa_{1/3}NbO_3$ at the Electrode−Electrolyte Interface

Masanobu Nakayama, Hiromasa Ikuta, Yoshiharu Uchimoto, and Masataka Wakihara*

Department of Applied Chemistry, Tokyo Institute of Technology, Ookayama, Meguro-ku, Tokyo 152-8552, Japan

Received: July 16, 2003

Hereunder presented is an AC impedance spectroscopic study of the lithium-inserted material $Li_xLa_{1/3}NbO_3$. Two semicircles were noted in accordance with the plots given as the complex impedance in the frequency region of 0.5 to 5000 Hz at room temperature, and these two semicircles made variation accompanied with the composition *x*. The dependence of the impedance spectra on the lithium salt concentration and temperature was examined, and it is explained that these two semicircles were in relation to the Butler−Volmer type kinetics. The evolution of impedance spectra for various conditions reveals that the electrochemical insertion process is described in terms of an adatom model; the resistance observed at a higher frequency region includes the adsorption and desolvation process accompanied with electron-transfer reaction. Furthermore, assignment as lattice incorporation, or insertion process at the electrode surface, is made with the other one observed in the lower frequency region.

Introduction

Electrochemical lithium insertion technique is a method with particular significance to high-energy density electrode materials to be used for lithium ion batteries.[1−3] Materials having lithium insertion sites are attractive not only to be used for the practical purpose but also to be used as a model material in the fundamental study of solid-state electrochemical reactions. This stems from two reasons described as follows: (1) the host crystal structure remained almost unchanged before and after the electrochemical reaction,[4] and (2) the free energy of the reaction, the molar amount of reacted species, and kinetic parameters such as diffusion coefficient can easily be obtained by monitoring the cell voltage and electronic current through the theories of electrochemistry.[5] Therefore, materials prepared by electrochemical reaction are adequate enough to use in experimental and theoretical manners, and can provide such useful knowledge as crystal and electronic structure at an equilibrium state, ion diffusion properties with the reaction, etc.[2,3] However, the acquired knowledge was restricted to the extent of the bulk properties of the reaction. In comparison with the remarkable advancement in the field of bulk properties, the reaction mechanism, especially the one on the kinetic properties at the electrode−electrolyte interface, is still ambiguous, exclusively in the case of insertion reaction.

So far, kinetics of soluble redox systems and electroplating systems have been well established based on the theory of Buttler−Volmer type charge-transfer reaction,[5] and so on. On the other hand, the detailed mechanism of electrochemical reaction of solid/liquid interface is still uncertain due to the fact that the reaction is dependent on several elemental subreactions, which introduces a complexity directed toward the quantitative discussion. Such an electrochemical reaction at the solid/liquid interface is known as a key technology not only for the Li ion battery, but also for the fuel cell, Ni−H battery, electrochromism, corrosion, catalysis, and so on. Therefore, accurate knowledge of these processes is demanded for the sake of material and device design. One solution for this issue is the separation of elemental reactions by time-resolved experimental approaches, such as the AC impedance technique.[5,6] So far, numerous reports are available on the AC impedance measurement applied to the electrode reaction for lithium ion batteries,[7] but it is usually difficult to separate the elemental reaction because each elemental reaction has similar relaxation time at room temperature.

Recently, systematic study was made regarding the variation of bulk properties upon the lithium insertion reaction in the A-site deficient type perovskite oxides,[8−10] with a purpose to explain that these materials are adequate enough to be used for fundamental study of bulk properties while the lithium insertion reaction is in progress.[11,12] Through these observations, it is revealed that the material in question is proper enough for the basic study not only on the bulk reaction but also on the interface reaction. As will be reported in detail in the following sections, two pieces among the impedance components were successfully separated at room temperature. Thus, different behavior was shown with composition *x*. The present paper, which describes the behavior of two impedance components as functions of composition *x*, electrolyte concentration, and temperature, investigates the elemental reaction mechanism by the phenomenological interpretation.

Experimental Section

$La_{1/3}NbO_3$ was prepared in accordance with the conventional solid-state reaction. As described in ref 13, heating the mixture of stoichiometric amounts of La_2O_3 (3N) and Nb_2O_5 (3N) (Soekawa Chemical Industries, Limited) at 800 °C for 2h. After that, heating was furthermore made with several intermittent grindings at 1300 °C for 24 h in air.

Electrochemical reaction of Li insertion was achieved using a three-electrode cell. Li foil (Aldrich) was used as both counter

* Corresponding author. Tel.: + 81 3 5734 2145; Fax: +81 3 5734 2146.

10.1021/jp036059k CCC: $25.00
Published on Web 08/28/2003

and reference electrodes. Since the activity coefficient of the electrolyte exhibits deviation from the activity coefficient a proportional manner rather than c.a. 0.4 M as referred to in the section following this description, 0.2 M solutions of $LiClO_4$ in anhydrous ethylene carbonate (EC) and diethylene carbonate (DEC) were used as electrolyte (Tomiyama Pure Chemical Company, Limited), except for the case in some of the other experiments (detailed condition wsill be described at each section). The working electrode consisted of the mixture of 90 wt % perovskite powders, 7 wt % acetylene black as a current collector, and 3 wt % poly(tetrafluoroethylene) (PTFE) binder. The mixture was pressed into a film, and at the same time, a disk was cut out from the film. A typical working electrode was 3−4 mg in weight with a surface area of 0.2 cm^2, and its approximate thickness was 100 μm. Li foils and the mixture of working electrode were pressed onto Ni-mesh. To avoid complexity caused by the difference of surface area, the same electrode was used for the sake of the comparison with each experimental data (Note that most of electrochemical properties such as overpotential are the function of the current density). The all-electrochemical reaction was caused and measurement was made with the aid of Solartron 1287 potentiogalvanostat and 1255B frequency response analyzer. The preparation of the samples with various composition x was made by electrochemical reaction with slow current density, 40 $\mu A/cm^2$, and furthermore relaxed to the extent of the state in equilibrium. The impedance spectra were measured at frequencies ranging from 10^{-2} to 10^5 Hz. The preparation of the cells was performed in an Ar-filled glovebox. The electrochemical measurements were carried out in an airtight vessel filled with Ar gas, which allowed the cell from the glovebox to be removed. The vessel was placed in an incubator for the purpose of controlling the experimental temperature.

Crystalline phase identification for the $Li_xLa_{1/3}NbO_3$ was carried out by powder X-ray diffraction (XRD) using a Rigaku RINT2500V diffractometer with CuKβ radiation, a curved graphite monochromator. Thus it is confirmed that host−perovskite structure was kept unchanged through the reaction, and detailed reports concerning the above were already released elsewhere.[9,10]

Results

Compositional Dependence. Figure 1(a) shows the observed cell potential where impedance measurements were conducted (solid circle), and the potential is in good agreement with the equilibrium voltage of $Li_xLa_{1/3}NbO_3$ [8] (open symbol in Figure 1a), which is previously reported by us, the authors of this paper. Decrease is noted with the cell potential in the composition range of $0 < x < 0.6$ (solid solution reaction), and a plateau is shown on a boundary up to approximately $x > 0.7$ (two phase reaction). At the final stage, large polarization was observed at $x \sim 0.7$, indicating that the lithiation into perovskite oxides was terminated. Since the composition where the said termination occurred is consistent with the amount of vacancies at the perovskite A-site, the lithium ion insertion was made into the perovskite A-site.

A report concerning the details of lithiation process and structural analysis has already released.[8] Figure 1b shows the cell potential change of the first discharge (Li insertion) and charge (Li extraction) reaction at a very slow rate (40$\mu A/cm^2$). Reversible insertion of the lithium ions into the perovskite and extraction from the same were made, and it is explained that approximately 1% of inserted lithium exclusively corresponds to the irreversible capacity. Therefore, almost none of side

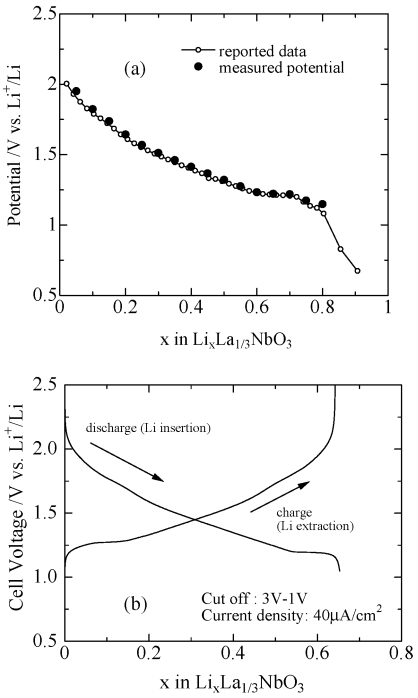

Figure 1. Variation of the potential with composition x in $Li_xLa_{1/3}NbO_3$. (a) Equilibrium cell potential; the open circles indicate the previous data (ref 8) of the equilibrium potential, and solid circles indicate the present data where the impedance spectra were measured. (b) Slow rate charge−discharge cell potential diagram.

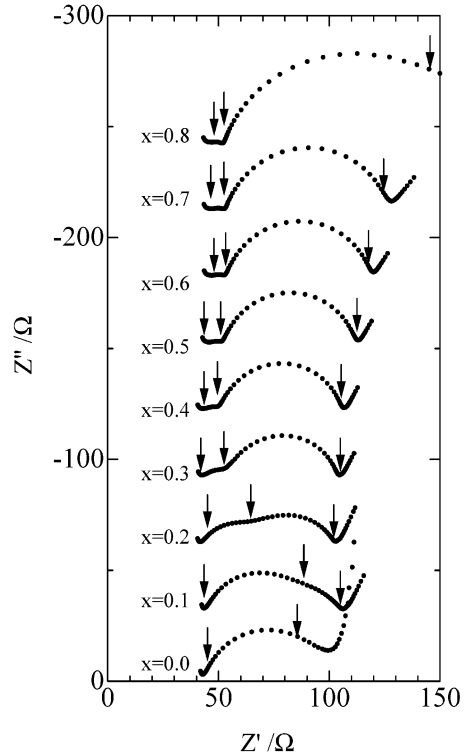

Figure 2. Complex impedance plots obtained at 30 °C at the various compositions of $Li_xLa_{1/3}NbO_3$. Arrows indicate the data obtained at 5000 Hz, 150 Hz, and 0.5 Hz, respectively.

reactions such as decomposition of organic solvent is to be seen here. Figure 2 shows the complex impedance plots at 30 °C as a function of the composition x in $Li_xLa_{1-x}NbO_3$. Two semicircles (referred to hereafter as "semicircle 1" for higher frequency and "semicircle 2" for lower one) were observed in a range of 0.5 Hz to 5000 Hz. (It is especially obvious that the

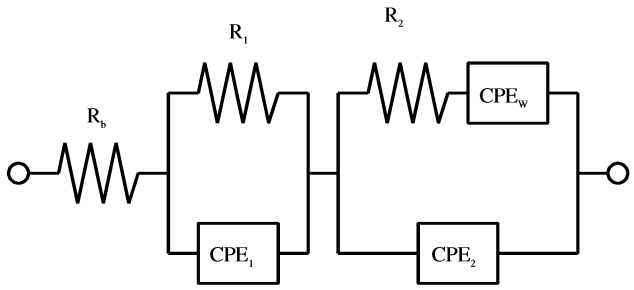

Figure 3. Equivalent circuits used for a curve-fitting procedure for the observed impedance spectra.

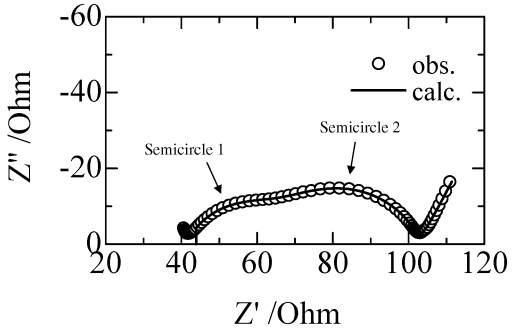

Figure 4. Typical results of curve-fitting procedure (solid line) in comparison with observed data (open symbol). Presented data is impedance spectra of the sample, $Li_{0.2}La_{1/3}NbO_3$, at 30 °C.

separation was observed at the composition around $x = 0.2$.) During the process of lithiation, the semicircle 1 was going to disappear because resistance was decreased. In the meantime, semicircle 2 became larger. To evaluate the variation of impedance spectra quantitatively, two circles were curve-fitted by using the equivalent circuit shown in Figure 3, where R_b is a bulk resistance of electrolyte. Meanwhile R_i and CPE_i denote the resistance and constant phase element (CPE) of semicircle i (i=1 or 2). The CPE is an empirical impedance function of the type, $Z^*_{CPE} = A(j\omega)^{-\alpha}$, which was in use replaced with capacitance by taking into account the rough nature of the electrode (the details of CPE were described in ref 6). Typical results of curve-fittings are presented in the Figure 4 showing a good agreement of the experimental with the calculated impedance spectra (goodness of fit, χ^2, is of the order of 10^{-5} for the composition $0 < x \leq 0.7$). The best results of fitted resistance are summarized in the Figure 5 as a function of composition x. Since the semicircle 1 almost disappeared at the composition $x > 0.4$ as shown in Figure 2, it is difficult to estimate the accurate value of the resistance R_1 and CPE_1. This makes it hard to further discuss these two components in the present paper. The resistance R_b is constant at about 45 Ω through the lithium insertion and is consistent with the bulk resistance of 0.2M $LiClO_4$ in EC+DEC solution, measured previously using the same three-electrode apparatus with symmetrical electrode system, Li|electrolyte|Li. Therefore R_b is assigned as the bulk resistance of the electrolyte. The resistance R_1 is monotonically decreasing with lithiation in a range of $0 < x < 0.4$ (Figure 5). On the other hand, the change of the resistance R_2 is contrary to that of R_1. In the final part of this paper, we will discuss the origin of the impedance components, R_1 and R_2.

Dependence on the Concentration of Electrolyte. The impedance behavior owing to the reaction at the electrode−electrolyte interface is generally interpreted as the reaction expressed by the Butler−Volmer type equation based on electron-transfer theories.[5] According to this equation, the

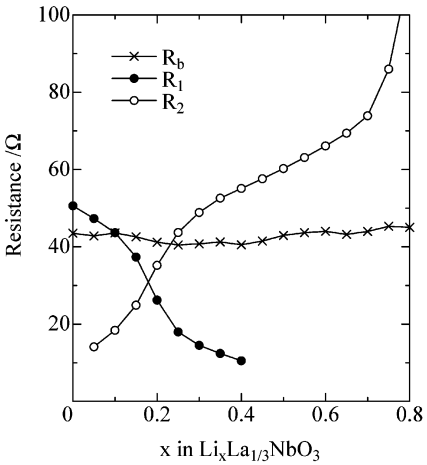

Figure 5. Variation of the each resistance obtained by curve-fitting procedure upon lithiation as a function of composition x. No plotting is made with the resistance R_1 with $x > 0.4$ because of low reliability of data (mentioned in the text).

exchange current i_0 is expressed as shown below.

$$i_0 = A \cdot a_{\mathrm{Li,liq}}^{1-\alpha} \cdot a_{\mathrm{Li,sol}}^{\alpha} \cdot \exp\left(-\frac{\Delta G^*}{RT}\right) \quad (1)$$

where $a_{Li,liq}$ and $a_{Li,sol}$ are the activities of lithium in electrolyte (liquid) and electrode (solid), respectively. A is the solvent-independent part of the preexponential factor. ΔG^* is the Gibbs activation energy of the electron-transfer reaction, and α is a transference coefficient, which usually is considered to be 0.5. The essence of the eq 1 is described in this manner. That is to say, the product of two activity components indicates the reaction is occurring at the two-phase interface, and the Boltzmann-type exponential term denotes a thermally activated type of reaction. Therefore, this expands to the extent of the other kind of elemental reaction occurring at electrode−electrolyte interface; although the equation originally assumes a single elemental reaction at the interface and electron-transfer reaction as the rate-determining process.

If the activity $a_{Li,sol}$ is constant and $a_{Li,liq}$ corresponds to the concentration of electrolyte in the low concentration range, then eq 1 is modified as follows:

$$i_0 = A' \cdot C_{\mathrm{Li,liq}}^{1/2} \cdot \exp\left(-\frac{\Delta G^*}{RT}\right) \quad (2)$$

where $C_{Li,liq}$ is a concentration of Li^+ in the electrolyte, and A' is a constant equal to the product of A and $a_{Li,sol}$.

To ascertain whether the present lithium insertion reaction can be applied to Butler−Volmer type reaction referred to above, investigation is made as to the dependence of the impedance spectra on the electrolyte concentration $C_{Li,liq}$. In this experiment, 0.1, 0.2, 0.3, 0.4, 0.5, 0.6, and 1.0 M solutions of $LiClO_4$ in anhydrous ethylene carbonate (EC) and diethylene carbonate (DEC) were used as electrolyte (Tomiyama Pure Chemical Company, Limited). The samples with the composition $x = 0.1$ and 0.6 were used as the working electrode to investigate the impedance behavior of semicircles 1 and 2, respectively, because of the following two reasons: (i) the activity of lithium in the electrode was fixed for the purpose of applying eq 2 as mentioned above, and (ii) the features of semicircles 1 and 2 are distinctly observed at the compositions $x = 0.1$ and 0.6, respectively (Figure 2). In addition, the same sample is used both for the compositions to keep the same surface area and for the electrode which was rinsed in EC+DEC solvent in

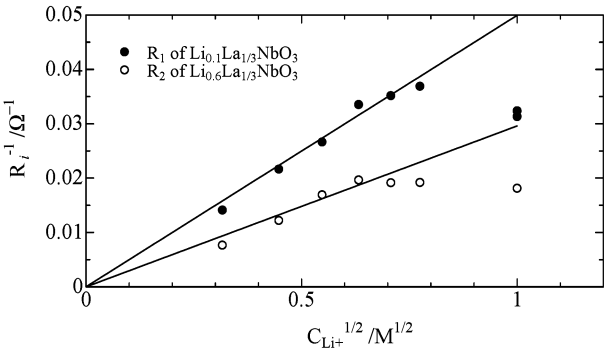

Figure 6. The dependence on the square root of the electrolyte concentration at 30 °C for inverse resistance R_i. The solid symbol indicates the obtained resistance R_1 for the sample, $Li_{0.1}La_{1/3}NbO_3$, whereas the open symbol indicates the R_2 for the sample, $Li_{0.6}La_{1/3}NbO_3$.

relation to every measurement. Since the exchange current i_0 for each elemental reaction is proportional to the inverse resistance R_1 and R_2, the obtained results were plotted as $1/R_i$ ($i = 1, 2$) with respect to the square root of electrolyte concentration $C_{\mathrm{Li,liq}}^{1/2}$, as shown in Figure 6. In the case of the sample with $x = 0.1$, which represents the semicircle 1, a linear relationship between $C_{\mathrm{Li,liq}} = 0.1$ and 0.6 M is obtained and the other sample with $x = 0.6$ is also proportional to the square root of electrolyte concentration up to 0.4 M solution. Accordingly, both of the reactions observed as semicircles 1 and 2 may obey the Butler−Volmer type equation, indicating that the reactions manifest themselves at the electrode/electrolyte interface.

Temperature and Solvent Dependence. As referred to in the previous section, the elemental reaction seems to obey the Butler−Volmer type equation. This compels the inverse resistance $1/R_1$ and $1/R_2$ to exhibit the Arrhenius-type dependence on the temperature (see eq 1 or 2). With a view to ensuring the validity of this matter, measurement was made with the impedance spectra at various temperatures ranging from 30 to 60 °C. The changes of resistance R_1 and R_2 were measured at the composition $x = 0.1$ and 0.6, respectively, because the feature R_1 and R_2 are apparent at these compositions as described previously. Measurement was furthermore made with the impedance spectra, using two kinds of solvent, i.e., EC+DEC and propylene carbonate (PC). The results obtained from the above procedure were successfully plotted in accordance with the Arrhenius form, and they are illustrated in Figure 7. Since both of the resistances R_1 and R_2 obey the Arrhenius manner, the two reactions related to R_1 and R_2 correspond to the so-called thermal activation process. The activation enthalpy of the reaction, which is obtained from the slope of the plots, is tabulated in Table 1. The reaction associated with resistance R_1 has activation enthalpy relatively small in comparison with those observed at the resistance R_2. The smaller activation enthalpy may probably be caused because semicircle 1, observed in the higher frequency region, is associated with a rapid reaction. In addition, the activation enthalpy due to semicircle 1 exhibits dependence on the selection of solvents, while the activation energy observed in semicircle 2 tends to be independent of the solvent, EC+DEC or PC.

Discussion

The impedance behavior for the two-semicircle system of $Li_xLa_{1/3}NbO_3$ is quite a complicated one, and the reaction occurring at each semicircle is uncertain because of lack of information concerning the surface structure. Bruce and Saidi[14]

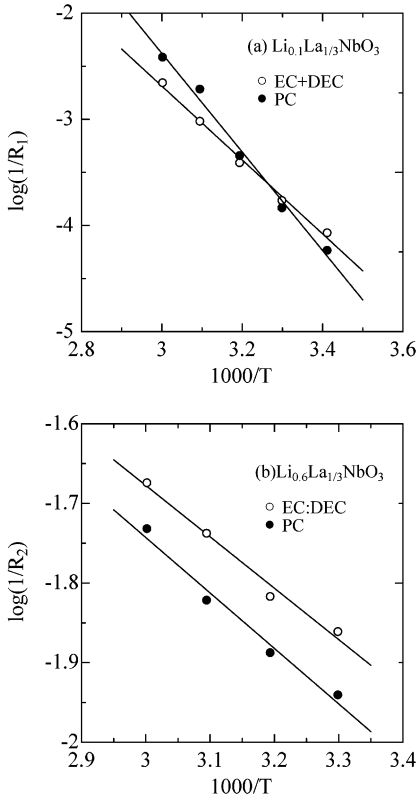

Figure 7. Plotting for $\log(1/R_i)$ vs inverse temperature at different intercalation degrees and solvents. (a) Plot of the resistance R_1 at the composition $x = 0.1$. (b) Plot of the resistance R_2 at the composition $x = 0.6$.

TABLE 1: Activation Enthalpy of Elemental Reactions Associated with Semicircles 1 and 2

electrolyte	semicircle 1 (at $x = 0.1$)	semicircle 2 (at $x = 0.6$)
0.2 M $LiClO_4$ in 1:1 EC+DEC	28.9 kJ/mol	53.6 kJ/mol
0.2 M $LiClO_4$ in PC	38.6 kJ/mol	57.9 kJ/mol

purport that initially, solvated ions in the electrolyte near the electrode surface should be subjected to partial desolvation and electron transfer from the electrode, resulting in formation of an atom adsorbed on the electrode surface (adatom). This adatom migrates on the surface to an insertion site. Meanwhile its remaining solvents depart from the adatom, and the adsorbed ions come to be fully incorporated into the electrode material. Therefore, applying this model to the results obtained this time makes it possible for the former process to correspond to the semicircle 1, and the one obtained later is allowed to correspond to the semicircle 2. However, none of the impedance spectra of Li_xTiS_2 showed compositional dependence that was observed in this attempt. In this section, discussion is made as to the validity of the adatom model in the case of $Li_xLa_{1/3}NbO_3$.

Since the activation enthalpy of semicircle 1 exhibits a dependence of the solvent, semicircle 1 includes in itself the desolvation process produced in the electrolyte. However, it is not energetically feasible enough for desolvation reaction to form a single free Li ion in the bulk of the electrolyte solution due to the instability expected in the charged bare lithium ion. For example, the binding enthalpy of the Li^+−carbonate system is −217.6 kJ/mol (EC) and −215.9 kJ/mol (PC) as reported by Blint,[19] or −232.6 kJ/mol (PC) as reported by Katayama et al.[20] (the values were estimated by ab initio molecular orbital calculation), and the values are large enough in comparison with the present result of activation enthalpy associated with semi-

circle 1 (38.6 kJ/mol for PC, 28.9 kJ/mol for EC+DEC in Table 1). Therefore, it is considered that along with the desolved lithium ions, formation is in progress in the chemical bonding with electrode surface ions to accomplish stabilization of the desolvated lithium ion. On the other hand, lithium desolvation simultaneously occurs with adsorption to the electrode surface. Nevertheless, the said assumption is not successful enough to explain that the resistance of semicircle 1 decreases upon lithium insertion, because the kinetics of these processes might be independent of composition x and concurrently might be dependent on the surface area. Considering the adsorption of Li^+ ion at the surface, the neutrality of electric charge fails to be kept locally. Therefore, the Li adsorption is liable to be produced around the surface O^{2-} ion in the vicinity of the Nb^{4+}, which is created by the electron-transfer reaction, $Nb^{5+} + e^-$, by maintaining the locally electrical neutrality. And this model also assigns the compositional dependence of the resistance to the semicircle 1, because the number of Nb^{4+} ions increases with composition x. Summing up the discussion, the reaction associated with semicircle 1 includes the three elemental reactions, i.e., adsorption, desolvation, and electron-transfer reaction, respectively.

On the other hand, the reaction associated with semicircle 2 seems to be independent of the solvent from the data of the activation enthalpy. Although the desolvation process contributed to both the semicircles in the adatom model of metal deposition, semicircle 1 exclusively included the desolvation process in the case of $Li_xLa_{1/3}NbO_3$. Therefore, it is concluded that the possible rate determining reaction is surface conduction of adatom and/or Li^+ insertion. The compositional dependence on the impedance spectra was supported by the explanation to be referred to at the final stage. R_2 is monotonically increasing up until the moment to filling up vacant A-site. Furthermore, abrupt increasing of the resistance was observed. Such a behavior seems to correspond to the amount of A-site vacancies at the surface, which decreases with the composition x. On the other hand, none of surface conduction seems to be affected by the composition, but it is mainly dependent on the size of surface area. Therefore, the dominant contribution of semicircle 2 is ascribed to the lithium insertion process, or lattice incorporation.

Based on the adatom model, two-semicircle behavior upon lithium insertion was successfully interpreted by phenomenological discussion. Accordingly, it is concluded that the elemental reactions for semicircle 1 were assigned as corporative reaction of Li adsorption, desolvation, and electron-transfer reaction, and on the other hand, for semicircle 2 were assigned as lithium insertion in the surface area. A schematic image of the reaction at electrode/electrolyte interface is illustrated in Figure 8.

Conclusion

The $Li_xLa_{1/3}NbO_3$ electrode has been proved to be an example adequate enough for the fundamental study on the interfacial phenomena occurring at the electrode/electrolyte interface. Especially, it is noted that the 'adatom model' can interpret the reaction process occurring at electrode/electrolyte interface without contradiction.

It is shown by the impedance spectra with various conditions that the reaction observed in the higher frequency region consists of the adsorption, desolvation and electron-transfer reaction. Meanwhile it is also shown that the reaction observed in the lower frequency region corresponds to the lithium insertion ranging from interface to bulk structure.

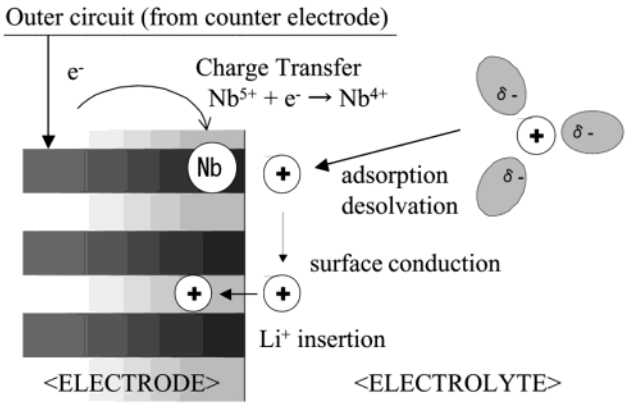

Figure 8. Schematic diagram of the lithium insertion reaction at electrode/electrolyte interface.

Acknowledgment. The authors wish to finalize this paper by confessing with their sincere gratefulness that this work was supported by Grant-in-Aid for Scientific Research on Priority Areas (B) (No.740) "Fundamental Studies for Fabrication of All Solid State Ionic Devices" from Ministry of Education, Culture, Sports, Science and Technology. One of the authors, M.N., particularly wishes to be thank the Japan Society for the Promotion of Science for their financial support accorded to this work. The authors' appreciation is extended to Ph.D. I. R. M. Kottegoda who has been kind enough to provide the authors with her precious advice and constructive suggestions.

References and Notes

(1) Scrosati, B. *Nature* **1995**, *573*, 557.
(2) Wakihara, M.; Guohua, L.; Ikuta, H. *Lithium Ion Batteries, Chapter 2*; Kodansha: Tokyo, 1998.
(3) Wakihara, M. *Mater. Sci. Eng.* **2001**, *R 33*, 109.
(4) In *Chemical Physics of Intercalation*; Legrand, A. P., Flandrois, S., Eds.; Plenum Press: New York, 1987.
(5) In *Electrochemical Methods, Fundamentals and Applications*; Bard, A. J., Faulkner, L. R., Eds.; John Wiley & Sons: New York, 2001.
(6) In *Impedance Spectroscopy, Emphasizing solid materials and systems*; Macdonald, J. R., Ed.; John Wiley & Sons: New York, 1987.
(7) For example; Nobili, F.; Tossici, R.; Marassi, R.; Croce, F.; Scrosati, B. *J. Phys. Chem. B* **2002**, *106*, 3909. Striebel, K. A.; Sakai, E.; Cairns, E. J. *J. Electrochem. Soc.* **2002**, *149*, A61. Krtil, P.; Fattakhova, D. *J. Electrochem. Soc.* **2001**, *148*, A1045. Dokko, K.; Mohamedi, M.; Fujita, Y.; Itoh, T.; Nishizawa, M.; Umeda, M.; Uchida, I. *J. Electrochem. Soc.* **2001**, *148*, A422. Dollé, M.; Orsini, F.; Gozdz, A. S.; Tarascon, J.-M. *J. Electrochem. Soc.* **2001**, *148*, A851. Chen, C. H.; Vaughey, J. T.; Jansen, A. N.; Dees, D. W.; Kahaian, A. J.; Goacher, T.; Thackeray, M. M. *J. Electrochem. Soc.* **2001**, *148*, A102.
(8) Nakayama, M.; Imaki, K.; Ikuta, H.; Uchimoto, Y.; Wakihara, M. *J. Phys. Chem. B* **2002**, *106*, *25*, 6437.
(9) Nakayama, M.; Imaki, K.; Ra, W.-K.; Ikuta, H.; Uchimoto, Y.; Wakihara, M. *Chem. Mater.* **2003**, *15*, 1728.
(10) Nakayama, M.; Ikuta, H.; Uchimoto, Y.; Wakihara, M.; Terada, Y.; Miyanaga, T.; Watanabe, I. *J. Phys. Chem. B* **2003**, in press.
(11) Nadiri, A.; Le Flem, G.; Delmas, C. *J. Solid State Chem.* **1988**, *73*, 338.
(12) Shan, Y. J.; Chen, L.; Inaguma, Y.; Itoh, M.; Nakamura, T. *J. Power Sources* **1995**, *54*, 397.
(13) Kawakami, Y.; Ikuta, H.; Wakihara, M. *J. Solid State Electrochem.* **1998**, *2*, 206.
(14) Bruce, P. G.; Saidi, M. Y. *J. Electroanal. Chem.* **1992**, *322*, 93.
(15) Gerischer, V. H. *Z. Elektrochem.* **1958**, *62*, 256.
(16) Fleischmann, M.; Rangarajan, S. K.; Thirsk, H. R. *Trans. Faraday Soc.* **1967**, *63*, 1240, 1251, 1256.
(17) Armstrong, R. D.; Henderson, M. *J. Electroanal. Chem.* **1972**, *39*, 81. Armstrong, R. D.; Firman, R. E. *J. Electroanal. Chem.* **1973**, *45*, 257.
(18) Hendrikx, J.; Visscher, W.; Barendrecht, E. *Electrochim. Acta* **1985**, *30*, 999.
(19) Blint, R. J. *J. Electrochem. Soc.* **1995**, *142*, 696.
(20) Katayama, H.; Arai, J.; Akahoshi, H. *J. Power Sources* **1999**, *81*−*82*, 705.